



Research Report

Intra-saccadic displacement sensitivity after a lesion to the posterior parietal cortex



Jasper H. Fabius^{a,b,*}, Tanja C.W. Nijboer^{a,c}, Alessio Fracasso^{b,d,e} and Stefan Van der Stigchel^a

^a Experimental Psychology, Utrecht University, Utrecht, the Netherlands

^b Institute of Neuroscience and Psychology, College of Medical, Veterinary and Life Sciences, University of Glasgow, Glasgow, Scotland, United Kingdom

^c Center of Excellence for Rehabilitation Medicine, Brain Center Rudolf Magnus, University Medical Center Utrecht, Utrecht University and De Hoogstraat Rehabilitation, Utrecht, the Netherlands

^d Radiology, Center for Image Sciences, University Medical Center Utrecht, GA, Utrecht, the Netherlands

^e Spinoza Center for Neuroimaging, University of Amsterdam, BK, Amsterdam, the Netherlands

ARTICLE INFO

Article history:

Received 27 June 2019

Reviewed 31 July 2019

Revised 20 December 2019

Accepted 28 January 2020

Action editor D. Samuel

Schwarzkopf

Published online 19 February 2020

Keywords:

Visual perception

Saccade

Visual stability

Stroke

Parietal cortex

ABSTRACT

Visual perception is introspectively stable and continuous across eye movements. It has been hypothesized that displacements in retinal input caused by eye movements can be dissociated from displacements in the external world using extra-retinal information, such as a corollary discharge from the oculomotor system. The extra-retinal information can inform the visual system about an upcoming eye movement and accompanying displacements in retinal input. The parietal cortex has been hypothesized to be critically involved in integrating retinal and extra-retinal information. Two tasks have been widely used to assess the quality of this integration: double-step saccades and intra-saccadic displacements. Double-step saccades performed by patients with parietal cortex lesions seemed to show hypometric second saccades. However, recently idea has been refuted by demonstrating that patients with very similar lesions were able to perform the double step saccades, albeit taking multiple saccades to reach the saccade target. So, it seems that extra-retinal information is still available for saccade execution after a lesion to the parietal lobe. Here, we investigated whether extra-retinal signals are also available for perceptual judgements in nine patients with strokes affecting the posterior parietal cortex. We assessed perceptual continuity with the intra-saccadic displacement task. We exploited the increased sensitivity when a small temporal blank is introduced after saccade offset (blank effect). The blank effect is thought to reflect the availability of extra-retinal signals for perceptual judgements. Although patients exhibited a relative difference to control subjects, they still demonstrated the blank effect. The data suggest that a lesion to

* Corresponding author. Experimental Psychology, Utrecht University, Utrecht, the Netherlands.

E-mail address: Jasper.Fabius@glasgow.ac.uk (J.H. Fabius).

<https://doi.org/10.1016/j.cortex.2020.01.027>

0010-9452/© 2020 The Authors. Published by Elsevier Ltd. This is an open access article under the CC BY-NC-ND license (<http://creativecommons.org/licenses/by-nc-nd/4.0/>).

the posterior parietal cortex (PPC) alters the processing of extra-retinal signals but does not abolish their influence altogether.

© 2020 The Authors. Published by Elsevier Ltd. This is an open access article under the CC BY-NC-ND license (<http://creativecommons.org/licenses/by-nc-nd/4.0/>).

1. Introduction

Eye movements (saccades) introduce brief disruptions and distortions to the inflow of visual information through the eyes. Yet, introspectively, most humans perceive a stable and continuous visual world. It has been hypothesized that perceptual continuity across eye movements is related to ‘remapping of receptive fields’ of visual neurons (Cavanaugh, Berman, Joiner, & Wurtz, 2016; Crapse & Sommer, 2012; Mirpour & Bisley, 2016). This neuronal property is defined as a modulation of the response profile to visual stimuli (retinal information) by neural signals that carry information about eye movements (extra-retinal information). Remapping of receptive fields was first discovered in the lateral intraparietal sulcus of the macaque (Duhamel, Colby, & Goldberg, 1992), and later in other areas such as the superior colliculus (Walker, Fitzgibbon, & Goldberg, 1995), V4 (Tolias et al., 2001), and the frontal eye fields (Umeno & Goldberg, 1997).

These discoveries sparked interest in the behavioral consequences of a lesion to areas where neurons exhibit remapping properties. The hypothesis was that extra-retinal signals are either not available or not used appropriately after a brain lesion and therefore remapping of retinal information would be disrupted (Duhamel, Goldberg, FitzGibbon, Sirigu, & Grafman, 1992; Heide, Blankenburg, Zimmermann, & Kömpf, 1995). To test this hypothesis behaviorally, subjects with lesion affecting the frontal lobe or posterior parietal cortex (PPC) were asked to perform double step saccades (Hallett & Lightstone, 1976). In this task, two flashes of light are presented briefly in sequence. Subjects are asked to make two saccades, from the initial fixation point to the first target and then on to the second target. The rationale for using this paradigm to test for remapping is that the location of the second target must be updated after the first saccade. The retinal location of the second target cannot be used to execute the second saccade because it is not appropriate anymore after the first saccade, i.e., the retinal location of the second target has to be remapped based on the vector of the first saccade. Two studies indeed provided evidence that subjects with lesions to the PPC exhibit hypometric second saccades when the first saccade was directed to the contralesional side (Duhamel, Goldberg, et al., 1992; Heide et al., 1995). Later, the same observation was made for patients with a thalamus lesion (Bellebaum, Daum, Koch, Schwarz, & Hoffmann, 2005; Ostendorf, Liebermann, & Ploner, 2010). However, recently, the two studies focusing on PPC lesions have been criticized for two main reasons (Rath-Wilson & Guitton, 2015). In the study of Rath-Wilson and Guitton (2015), six patients with nearly identical lesions as the patients in the older studies performed the same double-step

saccade task and two other variation thereof. The first criticism was that the trial exclusion criteria were too conservative in the older studies. Although the second saccade was hypometric according to the original analysis, these saccades tended to be followed by one or more saccades bringing the fixation location close to the second target. When analyzing this ‘composite second saccade’, performance was on par with controls. The second criticism was that the classic double step task can be confusing, and subject tend to mix up the order of the two targets. With two variations on the classic double step task, where this problem was circumvented, patients performed again on par with controls. Hence, extra-retinal signals seem to guide saccades after a lesion to the PPC.

Double step saccades assess the accuracy and precision of extra-retinal signals for motor control, but not for perception. To directly assess the influence of extra-retinal signals on perception, the intrasaccadic displacement task has been used in both humans (Bridgeman, Hendry, & Stark, 1975; Deubel, Schneider, & Bridgeman, 1996) and monkeys (Cavanaugh et al., 2016). This task has also been used in patients with thalamus lesions (Ostendorf et al., 2010; Ostendorf, Liebermann, & Ploner, 2013), but not yet in patients with PPC lesions. The intrasaccadic displacement task consists of two conditions. In the first condition (STEP), subjects are asked to make a saccade to a target when it appears. The saccade target is displaced during the saccade, and subjects are asked to indicate the direction of the displacement. In the second version (BLANK), the saccade target is removed during the saccade, and then reappears displaced 300 ms after saccade offset. In the STEP condition, surprisingly large displacements go unnoticed to an observer, with thresholds around 30% of the saccade amplitude. However, the temporal gap between saccade offset and target onset in the BLANK condition increased detection sensitivity, with thresholds around 10% of the saccade amplitude (Deubel, Bridgeman, & Schneider, 1998; Deubel et al., 1996). We refer to this increase in sensitivity with the ‘blank effect’. The failure to detect a displacement in the STEP condition suggests that subjects primarily use visual information rather than extra-retinal information in trans-saccadic perception (Deubel et al., 1998; see also; Fabius, Fracasso, & Van der Stigchel, 2016). However, the availability and use of extra-retinal signals is highlighted by the blank effect. In other words, the increase in sensitivity from the STEP condition to the BLANK condition indicates the availability of extra-retinal information for perceptual judgements.

The blank effect has been used to study impairments in extra-retinal signals after stroke in human patients. Patients with thalamus lesions demonstrated a sensitivity decrease instead of increase from the STEP to the BLANK condition, i.e.,

they performed worse when they had to rely on extra-retinal signals (Ostendorf et al., 2010, 2013). Although no studies have used this task in patients with PPC lesions, there are two studies that have assessed location memory across saccades with a more cognitive task (Russell et al., 2010; Vuilleumier et al., 2007). Subjects with right hemisphere lesions were instructed to keep the location of a peripheral stimulus in memory and make a saccade such that the memorized location moved from the left to right visual field (or vice versa). After a delay, a second stimulus appeared either at the same location or displaced from the remembered location. Sensitivity was abnormally low when the stimulus was moved from the right to the left visual field, with an ipsilesional saccade (Russell et al., 2010; Vuilleumier et al., 2007). Although the time scale of this task differs from the intra-saccadic displacement task – and therefore putting more emphasis on working memory – their results suggest that spatial memory is degraded after an ipsilesional saccade in patients with PPC lesions.

Here, we test the hypothesis that lesions to the PPC specifically affect the integration of retinal and extra-retinal signals for perception using the intrasaccadic displacement task. If the hypothesis is correct, then a lesion to the PPC should result in a decreased sensitivity in the BLANK condition as compared to the STEP condition, similar to the human patients with thalamus lesions (Ostendorf et al., 2010, 2013). Neurophysiological evidence suggests that neurons in the PPC are important for the integration of retinal and extra-retinal signals for visual perception (Duhamel, Colby, et al., 1992; Mirpour & Bisley, 2016; Subramanian & Colby, 2014). In contrast, evidence from patients with PPC lesions demonstrates that the PPC is not crucial for the use of extra-retinal signals in motor control (Rath-Wilson & Guitton, 2015). The use of extra-retinal signals for motor control seems to be related more to the functioning of a network between the thalamus and the frontal eye fields (Ostendorf et al., 2010; Sommer & Wurtz, 2002, 2006). Possibly, lesions to the PPC specifically affect the integration of retinal and extra-retinal signals for perception, but not for motor control.

2. Materials and methods

This study was conducted in accordance with the principles of the Declaration of Helsinki (WMA) and the Dutch “Medical research involving human subjects” act. The procedures of this study were preregistered, reviewed and approved by the Medical Ethical Committee of the UMC Utrecht. All changes to the preregistered procedures are transparently identified. The approved registration form can be found on the Dutch CCMO website with file number NL53043.041.15: https://www.toetsingonline.nl/to/ccmo_search.nsf/fABRpop?readform&unids=9527EC8B5994F868C125847F0021B9E0. We report how we determined our sample size, all data exclusions, all inclusion/exclusion criteria, whether inclusion/exclusion criteria were established prior to data analysis, all manipulations, and all measures in the study.

2.1. Subjects

12 patients in the chronic phase post-stroke onset (>4 months) with chronic stroke damage and 30 healthy control subjects participated. These sample sizes were determined as the maximum possible given available resources. Patients were invited for participation after inspection of their clinical imaging data (MRI or CT scan) from existing databases at the UMC Utrecht that are available for scientific purposes. This database contains patients who had been admitted because of (suspected) cerebrovascular problems. Patients included in this database provided informed consent to have their imaging data be inspected for scientific purposes. Patients were included in the current study when there appeared to be a lesion to the right posterior parietal cortex (PPC). In practice, the right PPC was defined as lesions found A) posterior to the postcentral gyrus, B) dorsal to the posterior horn of the right lateral ventricle and C) not posterior to the parieto-occipital sulcus. Later, lesion locations were determined exactly by an expert neurologist. Patients were not included when they had exhibited clinical signs of visual field defects, a history of substance abuse, or an inability to understand the task instructions. See Table 1 for the demographic data of all patients and a summary of the healthy controls.

2.2. Lesion location

Lesions were drawn by a trained neurologist and projected to the MNI-152 anatomical template using MRICron (Rorden & Brett, 2000). We parcellated the posterior parietal cortex into four anatomically defined areas with the Automated Anatomical Labeling atlas (Tzourio-Mazoyer et al., 2002) available in MRICron. We defined the PPC to comprise the superior parietal lobule (SPL), inferior parietal gyrus (IPG), supramarginal gyrus (SGM) and angular gyrus (AG). For the entire PPC and each subarea, we computed the percentage of lesioned voxels of the MNI-template in MATLAB. These data are summarized in Table 1.

2.3. Experimental setup

Stimuli were displayed on a 48.9° by 27.5° Asus RoG Swift PG278Q, an LCD-TN monitor with a spatial resolution of 52 pixels/° and a temporal resolution of 120 Hz (AsusTek Computer Inc., Taipei, TW) in a darkened room, located 70 cm in front of the subject. The ultra low motion blur backlight strobing option of the monitor was disabled. Subjects rested their head on a chin-head rest, attached to the table. Eye position of the left eye was recorded with an Eyelink 1000 at 1000 Hz (SR Research Ltd., Mississauga, ON, Canada). The eye-tracker was calibrated using a 9-point calibration procedure. All stimuli were created and presented in MATLAB 2016a (The Math Works, Inc., Natick, MA.) with the Psychophysics Toolbox 3.0 (Kleiner et al., 2007) and the Eyelink Toolbox (Cornelissen, Peters, & Palmer, 2002). Visual onsets and eye-movement data were synchronized offline based on independent photodiode measurements (Fabius, Fracasso, Nijboer, & Van der Stigchel, 2019). To this end, we added 11 ms to the

Table 1 – Demographics. The rows ordered according to 1) PPC damage and 2) lesion volume.

ID	Age ^a	Sex ^b	Modified ^c	Years since CVA	Scan	Lesion volume (ml) ^d	Percentage damaged ^e				
			Rankin Scale (after 3 mo)				PPC (54.1 ml)	SPL (14.3 ml)	IPG (10.4 ml)	SMG (16.0 ml)	AG (13.3 ml)
L	55	0	2	1.85	CT	167.2	51.97	.08	41.06	94.80	64.99
A	65	0	3	4.43	MRI	187.6	47.08	2.93	43.53	93.18	42.14
C	76	1	1	5.43	CT	48.2	25.47	54.79	20.51	.04	28.29
K	47	1	2	6.10	MRI	37.2	23.69	56.16	36.59	2.18	4.44
D	57	1	2	2.53	MRI	26.4	14.12	0	8.28	42.42	0
I	41	0	1	5.92	MRI	47.5	12.97	0	.80	20.80	27.05
H	63	0	2	3.48	CT	64.2	5.05	0	0	14.39	3.26
M	59	1	2	.34	MRI	6.6	4.77	0	5.71	0	14.88
J	48	0	2	5.91	MRI	1.4	.91	.01	3.41	.84	0
E	51	0	0	4.17	MRI	57.4	0	0	0	0	0
B	81	1	2	1.90	MRI	.9	0	0	0	0	0
F	75	0	3	5.15	MRI	—	—	—	—	—	—
Average ^f	56.8	.44	1.89	4.00	-	65.2	20.67	12.66	17.77	29.85	20.56
Controls	51.3 [35, 66]	.43	-	-	-	-	-	-	-	-	-

^a For the controls the average is noted, and the min and maximum individual values are noted between brackets.

^b 0 = female, 1 = male.

^c The modified Rankin scale ranges from 0 (no symptoms) to 6 (dead).

^d Lesion volume in ml in the MNI-152 template.

^e PPC = posterior parietal cortex, SPL = superior parietal lobule, IPG = inferior parietal gyrus, SMG = superior marginal gyrus AG = angular gyrus.

^f The average is the average of subjects with lesions to the PPC (i.e., not subject E, B or F).

timestamps in the Eyelink data files that indicated visual onset during the experiment. This lag of 11 ms is most likely caused by input lag of the monitor and similar in magnitude to measurements by another group (Zhang et al., 2018).

2.4. Intrasaccadic displacement (Fig. 1A)

2.4.1. Task

Fixation targets were gray circles (13.01 cd/m², $\phi = .5^\circ$) with a superimposed black cross (line width = .15°) and gray point (Thaler, Schütz, Goodale, & Gegenfurtner, 2013), presented on a black background (.06 cd/m²). A stimulus appeared after a period of stable fixation (randomly sampled from the uniform distribution on the open interval [500, 1000] ms). Stimuli were red circles (5.40 cd/m², $\phi = .5^\circ$) presented 10° to the left or to the right of the fixation target, on the same horizontal axis as the fixation target. Subjects made a saccade towards the stimulus. When gaze was detected within a radius of 8° around the target, the stimulus was either displaced on the horizontal axis (STEP condition) or it disappeared for 300 ms and was displaced when it reappeared (BLANK condition). Subjects indicated the direction of the displacement by pressing the left or right arrow key on a standard keyboard. When no responses or no saccade was detected after 10 s, the trial was aborted and later repeated. Trials were divided into block of 32 trials. We collected as many trials as possible for patients within a time limit of 2 h including breaks. At the end of each block (~5 min) the screen slowly ramped up to full luminance, at the end of which the experimenter turned on the room light. This was done to prevent dark adaptation, which would make visual landmarks, such as the screen edge or eye tracker, more visible. Yet, even if these landmarks were visible, they are expected to contribute little to localization performance (Deubel, 2004).

2.4.2. Adaptive range of displacements

The displacement size varied from trial to trial and was sampled (without replacement) from a set of 32 displacement sizes that was compiled at the start of each block. This set was based on performance in all preceding blocks. In the first block, the displacement set was equal for all subjects, consisting of two repetitions of 15 linearly spaced displacements ranging from -5.8° to 5.8° in the STEP condition and from -3.5° to 3.5° in the BLANK condition. Additionally, we added two displacements of 0 (i.e., no displacement) to each set. Because we planned to fit psychometric function to the displacement data, we wanted to capture an appropriate range of displacements. However, we also wanted subjects to understand the task, and avoid confusion. To this end we implemented some adaptive variation to the limits of the displacement set. We adjusted the upper and lower limit of the displacement set after each block based on a simple logistic fit (i.e., only fitting the slope and offset, but keeping the asymptotes fixed to 0 and 1). The limits were set to the estimated displacement size to get to a performance of .99 and .01. The upper limit was constrained to be $\leq 7.5^\circ$, the lower limit was constrained to be $\geq -2^\circ$. In addition to the 30 linearly spaced displacements in this range (15 unique values repeated twice), we added two displacements of zero to each block, like in the first block. With these constraints we ensured that each block contained trials with leftward and rightward displacements, and trials without any physical displacement.

2.5. Analysis

2.5.1. Preprocessing

Saccades were detected with the algorithm by Nyström and Holmqvist, with a minimum saccade duration of 10 ms, a minimum fixation duration of 40 ms (Nyström & Holmqvist,

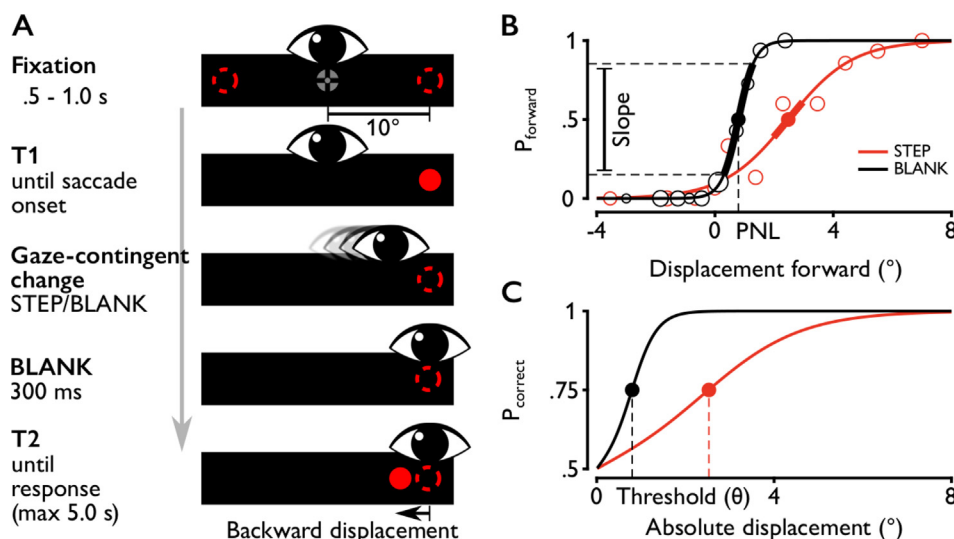


Fig. 1 – Experiment methods and example results. A. Trial sequence in the BLANK condition. Target size is not to scale. The BLANK was absent in the STEP condition, instead T2 (or, the displaced target) appeared during the gaze-contingent change. Displacements could be forward or backward with respect to the saccade direction. B. Example psychometric function of the STEP (red) and BLANK (black) condition for leftward saccades of one control subject. Circles represent the average proportion ‘forward’ responses in a bin. The size of the circles scales with the number of trials in that bin. Lines represent the fitted psychometric functions. The psychometric functions were fitted with two free parameters: the mean and the width. From the fits, we derived the perceptual null location (PNL) and slope. The PNL is the displacement at which the probability of a ‘forward’ response is the same as a response ‘backward’. The PNL is a measure of bias. The slope is the rate of change in proportion ‘forward’ per degree displacement at the PNL. The slope is a measure of sensitivity. C. In line with previous studies (Ostendorf et al., 2010, 2013), we also converted the psychometric functions to proportion correct. We defined the threshold (θ) as the absolute displacement where performance was .75 correct. The threshold captures a combination of bias and sensitivity.

2010). To ensure the online gaze-contingency worked adequately, all trials were visually inspected by plotting the x coordinate, y coordinate, velocity profile and x-y gaze path, with markings for the timing of visual on- or offsets. Trials where saccade latency was <80 ms, saccade amplitude was $<2^\circ$, eye velocity was $<150^\circ/\text{s}$ or the difference between saccade offset and T1 offset was <10 ms were highlighted to the inspector. The median percentage of exclude trials was 2.7% (min, max = 0%, 21.3%) for controls and 6.4% (min, max = 1.4%, 33.3%) for patients with PPC lesions. Moreover, trials where response time <200 ms or >5000 ms were removed automatically (5.3% for controls, 7.2% for patients).

2.5.2. Psychometric functions

We fitted a logistic function with two free parameters (mean and width) to the proportion ‘forward’ responses as a function of displacement size using Psignifit 4.0 (Schütt, Harmeling, Macke, & Wichmann, 2016). We fitted four psychometric functions, one per condition (STEP, BLANK) and saccade direction (left, right). Fig. 1B shows example fits for the STEP and the BLANK condition for one subject for leftward saccades. To estimate overdispersion, we computed the deviance for each psychometric function (four per participant) and the observed binned responses and compared the observed deviance to a bootstrapped distribution ($N = 2 \times 10^5$, Wichmann & Hill, 2001). From the psychometric function we calculated the perceptual null location (PNL) as the displacement where the proportion forward is equal the proportion backward

response. The PNL is a measure of bias, that can be either a perceptual bias or a response bias. In addition, we calculated the slope of the psychometric function at the PNL. The slope is a measure of sensitivity, higher slopes indicate a higher sensitivity to different displacement sizes. Following Ostendorf et al. (2010, 2013), we converted the fits to proportion correct as a function of the absolute displacement size (Fig. 1C). Next, we defined the threshold (θ) as the absolute displacement where performance equals a proportion of .75 correct. This measure captures the unsigned PNL and the slope of the function simultaneously and has been used in previous studies (Ostendorf et al., 2010, 2013).

2.5.3. Statistics

We performed two analyses, one confirmatory and one exploratory. For the confirmatory analysis, we tested the hypothesis that damage to the PPC impairs behavioral performance that relies on extraretinal signals. Here, behavioral performance is operationalized as the difference in slopes between the STEP and the BLANK conditions (see Psychometric functions). Following this hypothesis, the difference in slopes should be smaller for patients than for controls. In addition, there could be a difference between saccade directions, with a more pronounced deficit (i.e., smaller slope difference) for contralesional (i.e., leftward) saccades. We analyzed the slopes, as well as the PNLs and thresholds, using Bayesian mixed-design ANOVAs, with within-subject predictors ‘condition’ (STEP/BLANK), ‘direction’ (left/right) and between-

subject prediction ‘group’ (patient/control). The analysis was performed in JASP, using the default prior scales (.5 for fixed effects and 1.0 for random effects). Bayes Factors were computed with the Savage–Dickey density ratio across matched models. In an exploratory analysis, we analyzed the relationships between damage in specific subregions of the PPC and the slopes. These relationships were assessed using Bayesian interpretations of Kendall rank correlations, with a stretched beta prior with width = 1, one-sided tested for negative correlations (van Doorn, Ly, Marsman, & Wagenmakers, 2018).

2.5.4. Bayesian hierarchical model

In addition to the traditional fitting of psychometric functions, we also modelled the data with a Bayesian logistic linear mixed-effects model (see [Supplemental Material](#)). In this model the response on each trial is modelled as Bernoulli trial, with the probability of a ‘forward’ response given by a linear combination of condition (STEP/BLANK), saccade direction (left/right) and displacement size (degree in saccade direction). The parameters for these variables were sampled for each participant individually (subject parameters), that in turn were sampled from a hyperparameter that describes the distribution of each parameter at the population level (hyperparameters). For control, subjects, each parameter was sampled from two hyperparameters, one that reflects the mean of the population (μ) and one that describes the variation in the population (σ). For patients, a third hyperparameter was added to the mean, reflecting the average difference between patients and controls on that subject-specific parameter (δ). Because the number of patients was low ($n = 9$), we keep all σ 's the same for patients and controls. This means that we assume the variation among control subjects is approximately the same as the variation among patients. The benefit of the hierarchical structure over the individual fits is that the individual parameters estimates are now informed by the hyperparameters, because they serve as priors for the individual parameters. This means that for the parameter estimates of patients for whom we were not able to collect a lot of data (e.g., patient A), we do not have to rely solely on their data, but can also benefit from all other trials that the other participants completed.

3. Results

3.1. Demographics

Of the twelve subjects included based on an initial inspection of the available medical imaging data, nine subjects had a lesion in the PPC ([Fig. 2](#)). Patient E had extensive bilateral lesions that cover the superior frontal lobes but did not extend entirely to the PPC. Patient B only had two small lesions, with one in the white matter tracts beneath the PPC. Although Patient F had multiple lesions, the available scans were not suitable for manual labeling of the lesion. We will further discuss the performance of the other patients relative to the controls, without including patient B, E and F. Still, the psychometric functions of patient B, E and F can be found in the [Supplemental Material](#). The group of patients with PPC lesions

did not differ substantially in age ($BF_{10} = .863$) or female-male ratio ($BF_{10} = .327$) from the group of controls.

3.2. Psychometric functions

3.2.1. Quality of fit

Because we constrained data collection to a time limit rather than a trial limit, we could not anticipate the number of trials per condition or saccade direction. Still, we needed to fit four psychometric functions on the available data: for leftward and rightward saccades in the STEP and in the BLANK conditions. For all control subjects we had on average 189 trials per function (min = 93, max = 251). For patients, we had 123 trials on average. However, for patient A we had only 39 and 42 trials for leftward saccades in the STEP and BLANK condition, respectively. For F we only had 47 and 46 trials in the STEP condition for left- and rightward saccades respectively. Therefore, the data from these patients in these conditions should be interpreted with caution. In all other cases we had more than 100 trials per condition and saccade direction to estimate the parameters of the psychometric function. All estimated psychometric functions are displayed in [Figure S1](#). The quality of the fits was assessed by comparing the deviance of the fitted function to a bootstrapped distribution of deviances. Overall the deviance of the logistic functions was within the 95% confidence interval of the bootstrapped deviances (142/156 fits, 91%). We observed possible underdispersion in one of the fits of nine controls and one patients (C), and possible overdispersion in one of the fits of four control subjects. These results show that the logistic functions were, on average, a good fit to the data.

3.2.2. Displacement detection

The perceptual null locations (PNL) and slopes derived from the fitted logistic functions are displayed in [Fig. 3](#) and [Table S1](#). Parameter estimates obtained with the Bayesian model were in line with PNL and slopes reported here. However, estimates for the slope tended to be shallower for subjects with very steep slopes (particularly in the BLANK condition). This discrepancy is discussed in the [Supplemental Material](#). Thresholds are displayed in [Figure S2](#) and [Table S2](#). We tested for differences in PNL, slopes and thresholds using a Bayesian mixed-design ANOVA, with the factors group (patient/control) condition (STEP/BLANK) and saccade direction (left/right). For this analysis we took the log transformed thresholds. The data provide strong evidence for steeper slopes ($BF_{10} = 6.01 \times 10^{25}$) and lower thresholds in the BLANK condition than in the STEP condition ($BF_{10} = 4.34 \times 10^{12}$). These differences capture the blank effect ([Deubel et al., 1996](#)). In addition, there was evidence for a main effect of ‘group’ on the thresholds ($BF_{10} = 11.1$), but inconclusive evidence for this main effect on the slopes ($BF_{10} = .922$). More importantly, the data are suggestive of an interaction between condition and group on both the slopes ($BF_{10} = 7.85$) and thresholds ($BF_{10} = 7.14$). For both parameters, the effect of the blank is slightly stronger in the control group than in the nine patients with PPC lesions. For other interactions and main effects, the data were more likely under the null hypothesis than under the alternative (all $BF_{10} < .39$). The data were also more in favor of an absence of any of the effects on the PNL (all $BF_{10} < .77$). Estimates of the

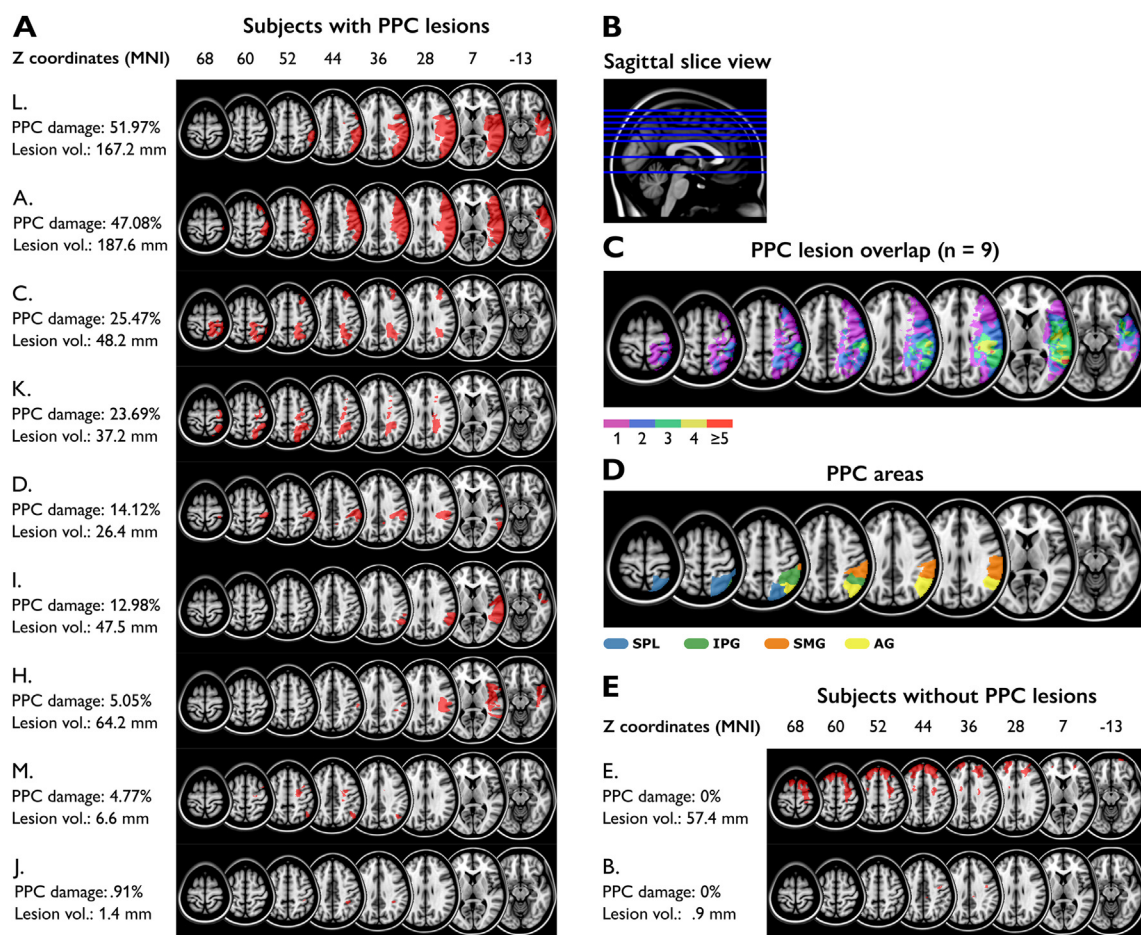


Fig. 2 – Lesions projected onto MNI template brain. **A.** Individual lesions of all subjects with lesions in the posterior parietal cortex (PPC). Subjects are ordered according to PPC damage and lesion volume. Percentage of damage is calculated based on location of the superior parietal lobule, inferior parietal gyrus, supramarginal gyrus and angular gyrus according to the Automated Anatomical Labeling atlas. **B.** Sagittal view of slices. Slices are chosen to facilitate the inspection of the PPC. **C.** Lesion overlap of the 9 subjects with lesions to the PPC. **D.** Areas that define the posterior parietal cortex (PPC) according to the AAL atlas. SPL = superior parietal lobule, IPG = inferior parietal gyrus, SMG = supramarginal gyrus, AG = angular gyrus. **E.** Individual lesions of the subjects without lesions to the PPC.

population parameters in the Bayesian model all point in the same direction as the ANOVA's (see [Supplemental Material](#)).

3.3. Correlation lesion and blank effect

As an exploratory analysis, here we correlate the percentage of damage to each of the four subareas of the PPC with the blank effect (i.e., the difference in slope between the BLANK and STEP condition). We use the Bayesian interpretation of Kendall's rank correlation for this analysis. Bayes Factors are computed for the one-sided hypothesis that more damage is related to a smaller blank effect. As we included only patients with right hemisphere lesions, we separated trials with leftward and rightward saccades. Please note that these correlations should only be interpreted as exploratory because there are only 9 subjects with PPC lesions in the current dataset. In general, the evidence for any correlation is between the blank effect and the percentage of damage in each region is low ([Fig. 4](#)), both in the direction of the null-hypothesis (no relationship) and in the direction of the alternative hypothesis

(negative relationship). For leftward saccades, there is some suggestive evidence for a relation between the amount of damage in the angular gyrus (AG) and the blank effect for leftward saccades ($\tau = -.48$, $BF_{10} = 3.20$). For rightward saccades, the strongest evidence was also for a correlation between the AG and the blank effect ($\tau = -.37$), however, the BF_{10} for this correlation is only 1.69, so inconclusive.

3.4. Saccade parameters

We analyzed the saccade parameters with Bayesian mixed-design ANOVA's, with the factors 'saccade direction' (left/right), 'condition' (STEP/BLANK) and 'group' (patient/controls). We added the main effects of condition, direction and the interaction between condition and direction to the null model. Bayes factors for the effects are computed across matched models. We report the average parameters per group and saccade direction, averaged over the two conditions. In the control group the median saccade latency ([Fig. 5A and D](#)) was 195 ms, 95%-CI = (139, 364) for leftward and 195 ms, 95%-CI =

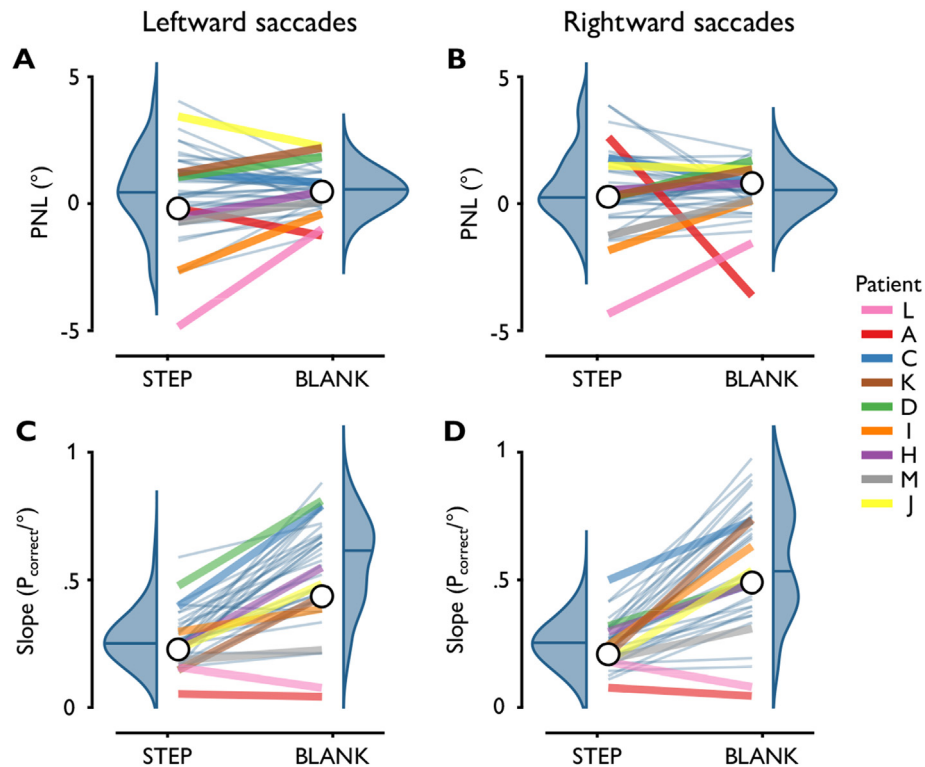


Fig. 3 – Displacement detection. A. Perceptual null location (PNL) for leftward saccades. B. PNL for rightward saccades. There is more evidence against than in favor of differences in PNLs between conditions, saccade directions or groups (all $BF_{10} < 1$). C. Slopes for leftward saccades. D. Slopes for rightward saccades. In each panel, the thin blue lines represent control subjects, the thicker colored lines represent the patients. Half, blue violins are the density distributions of the control subjects, with the median depicted as a horizontal line. The black circles depict the median of the patients. There is strong evidence for a difference in slopes between STEP and BLANK condition ($BF_{10} = 6.01 \times 10^{25}$) and suggestive evidence for a weaker BLANK effect in patients than in control subjects ($BF_{10} = 7.85$). For all other effect or interactions of group, condition and direction there was evidence against than in favor (all $BF_{10} < 1$).

(130, 334) for rightward saccades. In the patient group these latencies were 206 ms, 95%-CI = (164, 304) and 211 ms, 95%-CI = (183, 292), respectively. There was no evidence for an effect of any of the factors or their interactions on the saccade latencies (all $BF_{10} < .65$).

In the control group the median saccade amplitude (Fig. 5B and E) was 9.36° , 95%-CI = (7.52, 10.31) for leftward and 9.50° , 95%-CI = (6.91, 9.88) for rightward saccades. In the patient group these latencies were 9.21° , 95%-CI = (6.91, 9.88) and 9.40° , 95%-CI = (8.39, 10.02), respectively. These data show suggestive evidence for a main effect of direction, with leftward/centrifugal saccades being slightly more hypometric than rightward/centripetal saccades ($BF_{10} = 6.03$). This difference might be related to the observation that centripetal saccades (rightward here, because we measured the left eye in all subjects) tend to be slightly faster than centrifugal saccades (Collewyn, Erkelens, & Steinman, 1988). The velocity-based saccade detection algorithm we used for saccade detection could therefore have detected saccade endings slightly earlier in leftward than rightward saccades, resulting in the small difference in saccade amplitudes.

In the control group the median variation in saccade amplitude, defined as the standard deviation of the horizontal component of the saccade amplitude (Fig. 5C and F) was $.89^\circ$,

95%-CI = (.57, 1.22) for leftward and $.86^\circ$, 95%-CI = (.58, 1.32) for rightward saccades. In the patient group these latencies were $.98^\circ$, 95%-CI = (.72, 1.79) and $.82^\circ$, 95%-CI = (.73, 1.14), respectively. There was some suggestive evidence for an interaction between direction and group ($BF_{10} = 3.90$), with slightly more variability in leftward saccades for patients than for controls. There was no evidence an effect of any of the other factors or their interactions on the saccade amplitude variability (all $BF_{10} < .47$).

In addition to the saccades that were made in the displacement task, we also screened for visually guided oculomotor behavior in a brief screening task before the start of the experiment. In this task, subjects made saccades in 8 different directions starting in the center of the screen. As can be seen in Figure S3, there was no systematic difference in any of the eight directions concerning the latencies or amplitudes of the saccades.

4. Discussion

We measured the consequences of a lesion to the posterior parietal cortex (PPC) to the perception of intra-saccadic displacements. Saccades displace the entire visual field on the

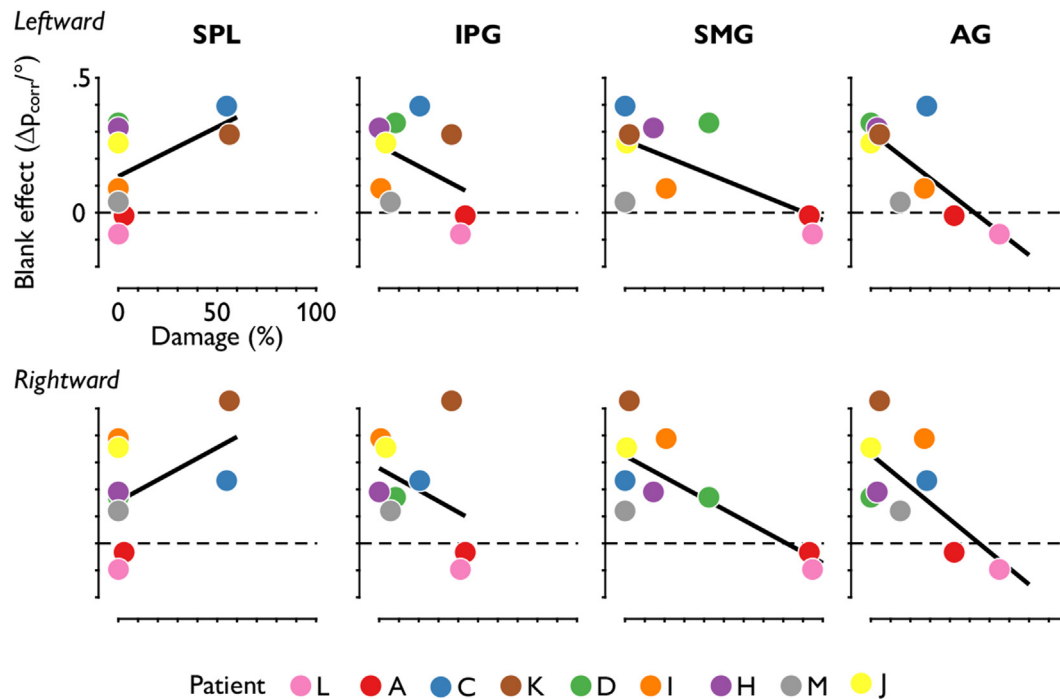


Fig. 4 – Correlation between the percentage of damage per subarea of the PPC and the blank effect (i.e., the difference in slope between BLANK and STEP condition). The upper row of panels contains the blank effect for leftward saccades, the bottom panels for rightward saccades. The black line is the least squares fit. SPL = superior parietal lobule, IPG = inferior parietal gyrus, SMG = supramarginal gyrus, AG = angular gyrus.

retina, yet these shifts go largely unnoticed to most humans. The major hypothesis of why the saccade induced shifts go unnoticed, is that the visual system can compensate/account for self-generated retinal shifts by monitoring extra-retinal signals, such as an efference copy from the oculomotor system. We used the intrasaccadic displacement task to measure the availability of such extra-retinal signals for perception in nine patients with lesions to the PPC. We measured reliable psychometric functions in both the STEP and BLANK condition of the intrasaccadic displacement task. We measured these conditions under the premise that a higher displacement sensitivity in the BLANK than in the STEP condition is indicative of monitoring extra-retinal signals (Deubel et al., 1996). We observed a small decrease in sensitivity for patients with a PPC lesions for displacements in the BLANK condition relative to control subjects. This indicates that extra-retinal information might not be as readily available as in control subjects. Still, most patients with substantial lesions to the PPC demonstrated the blank effect, i.e., behavior that indicates the influence of extra-retinal signals on their perceptual judgements.

These results lead to two primary conclusions. First, the PPC is indeed involved in monitoring a form of extra-retinal information or is part of one circuit that relays extra-retinal information, in line with previous studies that demonstrated that the PPC is involved in monitoring extra-retinal information for perception across saccades, in both humans (Dunkley, Baltaretu, & Crawford, 2016; Fairhall, Schwarzbach, Lingnau, Van Koningsbruggen, & Melcher, 2017; Medendorp, Goltz, Vilis, & Crawford, 2003; Merriam, Genovese, & Colby, 2003)

and monkeys (Duhamel, Colby, et al., 1992; Mirpour & Bisley, 2016; Subramanian & Colby, 2014). Second, after a lesion to the PPC the influence of extra-retinal information is lower, but not absent. Potentially, other sources of extra-retinal information (e.g., efference copy, eye proprioception, visual landmarks) or other circuits (e.g., superior colliculus, thalamus, frontal eye fields) can still provide the visual system with similar extra-retinal information. This alternative comes at a small cost, reflected in the slightly lower blank effect in patients than controls. Hence, the results of the current study do not support the hypothesis that the PPC is indispensable for monitoring extra-retinal information (Heide et al., 1995).

Our main hypothesis for the presence of the blank effect in patients with PPC lesions is the possibility that there are multiple neural circuits that could process extra-retinal information, i.e., degeneracy (Edelman & Gally, 2001; Price & Friston, 2002). This could mean that extra-retinal signals are processed in neural circuits that do not include the PPC, such as the thalamus and FEF (Sommer & Wurtz, 2008; Wurtz, 2008). For example, it has been proposed that perceptual continuity can be established by using an efference copy of the motor command as extra-retinal signals (von Holst & Mittelstaedt, 1950), but also by using proprioceptive signals from the eye (Steinbach, 1987; Sun & Goldberg, 2016). So far, the efference copy has been considered the most likely candidate, because a series of studies identified a network that relays an efference copy of the oculomotor command (Cavanaugh et al., 2016; Crapse & Sommer, 2012; Sommer & Wurtz, 2002, 2006). Moreover proprioceptive signals are thought to be slower than the

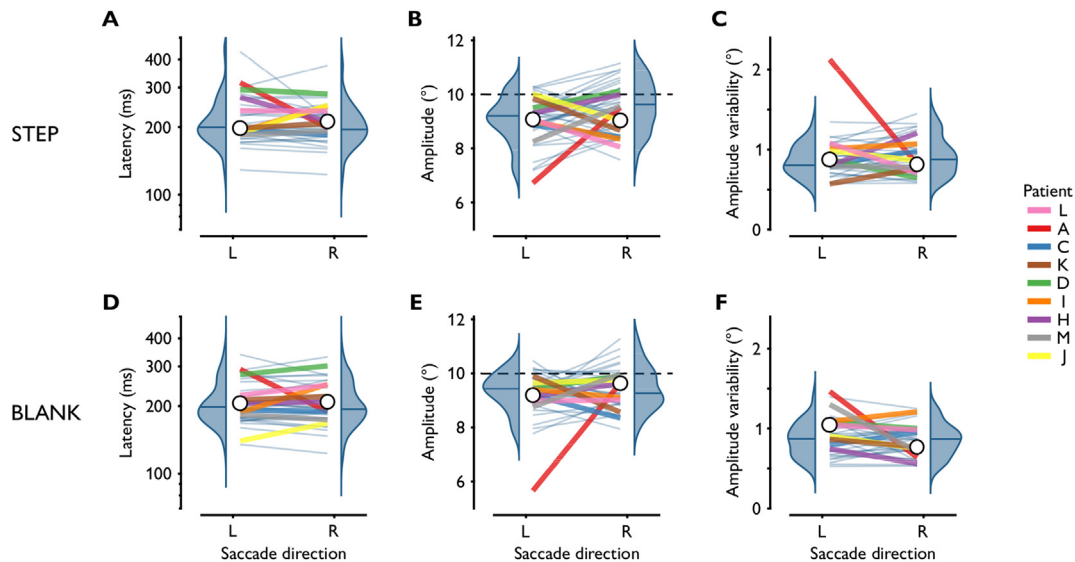


Fig. 5 – Saccade parameters. A-C. Median latency, average amplitude and amplitude variability in the STEP condition. D-F. The same parameters in the BLANK condition. Saccade variability in panels C and F is the standard deviation of the amplitudes of all trials included in the analysis per subject. In each panel, the thin blue lines represent control subjects, the thicker colored lines represent the patients. Half, blue violins are the density distributions of the control subjects, with the median depicted as a horizontal line. The black circles depict the median of the patients.

effference copy (Xu, Wang, Peck, & Goldberg, 2011, but see; Morris & Krekelberg, 2019) and are believed not to contribute to fast processes such as updating memorized saccade targets (Sparks & Mays, 1983; Sparks, Mays, & Porter, 2017). Still, proprioception guides motor control of eye movements over longer periods than single saccades (Poletti, Burr, & Rucci, 2013). The effference copy is believed to be the strongest extra-retinal signal across a single saccade, and is thus expected to contribute to perceptual continuity across saccades (Cavanaugh et al., 2016). However, proprioception of the eye provides an alternative, slower extra-retinal signal. Thus, hypothetically, if the PPC were crucial to integrating the effference copy with retinal information, patients with lesions to the PPC could still experience perceptual continuity when different and undamaged cortical areas integrate eye proprioception with retinal information.

A recent TMS study found evidence for a causal involvement of the PPC in the STEP condition of the intrasaccadic displacement task (Collins & Jacquet, 2018). Stimulation of the PPC with 3 pulse, 100 ms TMS resulted a forward shift of the PNL in the STEP condition for saccades contraversive to the TMS location. The BLANK condition was not measured in this study. Here, we use the relationship between the STEP and the BLANK condition to distinguish two scenarios. One in which extra-retinal information is completely abolished after a PPC lesion (i.e., no blank effect in the patients), and another one in which extra-retinal information is weighed differently after a PPC lesion (i.e., the blank effect is present but weaker). The current study adds to the findings of the TMS study, that the latter scenario is more likely than the former.

Together, the results of the current experiments provide a nuanced conclusion with regards to the involvement of the PPC in monitoring extra-retinal signals for perception. The main strength of the current study is the data quality. We

were able to collect sufficient data and good fits for the psychometric functions of most subjects, including the patients with substantial PPC lesions. The main limitation of the study is the relatively low number of patients, although it should be noted that nine patients with PPC lesions was not (much) lower than comparable studies on this topic (Heide et al., 1995; Rath-Wilson & Guitton, 2015; Russell et al., 2010; Vuilleumier et al., 2007). With this number, we could not perform lesion symptom mapping, which could be more sensitive to detect subtle lesion-deficit relationships.

5. Conclusion

To conclude, compared to healthy controls, patients with a chronic lesion to the PPC show a smaller blank effect on the intra-saccadic displacement task. This task has been used to study the influence of extra-retinal signals on visual perception across saccades in healthy humans, patients and non-human primates (Cavanaugh et al., 2016; Deubel et al., 1998; Ostendorf et al., 2010). Although the blank effect was smaller than in controls, most patients still showed a substantial increase in sensitivity as a result of the blank. If the blank effect is indeed an indication for the availability of extra-retinal signals for visual perception, then the current data suggest that patients with PPC lesions still have access to some form of extra-retinal signals. Therefore, the current results do not provide evidence for a crucial role of the PPC in monitoring extra-retinal signals for perceptual continuity, but, it could be that patients with a lesion to the PPC use a different source of extra-retinal signals than controls (e.g., eye proprioception instead of an effference copy). This difference comes at a small cost, reflected in the slightly lower blank effect in patients than controls. One example cost is the slower speed of

proprioceptive signals with respect to the efference copy. This leads to the hypothesis that perceptual continuity might only be disrupted after a PPC lesion when many saccades are in rapid sequence of each other.

Credit author statement

Jasper H. Fabius: Conceptualization, Methodology, Software, Validation, Data curation, Formal analysis, Visualization, Writing – Original draft, Project administration

Tanja C.W. Nijboer: Conceptualization, Writing – review & editing, Supervision, Funding acquisition

Alessio Fracasso: Methodology, Writing – review & editing, Supervision

Stefan Van der Stigchel: Conceptualization, Methodology, Writing – review & editing, Supervision, Project administration, Funding acquisition

Funding

This work was supported by a VIDI Grant 452-13-008 and a VENI Grant 451-10-013 from the Netherlands Organisation for Scientific Research awarded to Stefan Van der Stigchel and Tanja Nijboer, respectively. Alessio Fracasso is supported by grant BB/S006605/1 from the Biotechnology and Biological Sciences Research Council (BBSRC).

Data availability

All data, experiment scripts and analysis scripts are publicly available on Open Science Framework, DOI: 10.17605/OSF.IO/T5D36 (<https://osf.io/t5d36/>).

Open practices

The study in this article earned Open Materials, Open Data and Preregistered badges for transparent practices. Materials and data for the study are available at DOI 10.17605/OSF.IO/T5D36, p. 17.

Declaration of Competing Interest

The authors report no competing interest.

Acknowledgements

We thank Marjoleine Hakkenberg and Sinie van der Ben for their help in the data collection.

Supplementary data

Supplementary data to this article can be found online at <https://doi.org/10.1016/j.cortex.2020.01.027>.

REFERENCES

- Bellebaum, C., Daum, I., Koch, B., Schwarz, M., & Hoffmann, K. P. (2005). The role of the human thalamus in processing corollary discharge. *Brain: a Journal of Neurology*, 128(5), 1139–1154. <https://doi.org/10.1093/brain/awh474>.
- Bridgeman, B., Hendry, D., & Stark, L. (1975). Failure to detect displacement of the visual world during saccadic eye movements. *Vision Research*, 15(6), 719–722. [https://doi.org/10.1016/0042-6989\(75\)90290-4](https://doi.org/10.1016/0042-6989(75)90290-4).
- Cavanaugh, J., Berman, R. A., Joiner, W. M., & Wurtz, R. H. (2016). Saccadic corollary discharge underlies stable visual perception. *Journal of Neuroscience*, 36(1), 31–42. <https://doi.org/10.1523/JNEUROSCI.2054-15.2016>.
- Collewijn, H., Erkelens, C. J., & Steinman, R. M. (1988). Binocular co-ordination of human horizontal saccadic eye movements. *Journal of Physiology*, 404, 157–182. <https://doi.org/10/VL-404>.
- Collins, T., & Jacquet, P. O. (2018). TMS over posterior parietal cortex disrupts trans-saccadic visual stability. *Brain Stimulation*, 11(2), 390–399. <https://doi.org/10.1016/J.BRS.2017.11.019>.
- Cornelissen, F. W., Peters, E. M., & Palmer, J. (2002). The Eyelink Toolbox: Eye tracking with MATLAB and the Psychophysics Toolbox. *Behavior Research Methods, Instruments, & Computers*, 34(4), 613–617. <https://doi.org/10.3758/BF03195489>.
- Crapse, T. B., & Sommer, M. A. (2012). Frontal eye field neurons assess visual stability across saccades. *Journal of Neuroscience*, 32(8), 2835–2845. <https://doi.org/10.1523/JNEUROSCI.1320-11.2012>.
- Deubel, H. (2004). Localization of targets across saccades: Role of landmark objects. *Visual Cognition*, 11(2–3), 173–202. <https://doi.org/10.1080/13506280344000284>.
- Deubel, H., Bridgeman, B., & Schneider, W. X. (1998). Immediate post-saccadic information mediates space constancy. *Vision Research*, 38(20), 3147–3159. [https://doi.org/10.1016/S0042-6989\(98\)00048-0](https://doi.org/10.1016/S0042-6989(98)00048-0).
- Deubel, H., Schneider, W. X., & Bridgeman, B. (1996). Postsaccadic target blanking prevents saccadic suppression of image displacement. *Vision Research*, 36(7), 985–996. [https://doi.org/10.1016/0042-6989\(95\)00203-0](https://doi.org/10.1016/0042-6989(95)00203-0).
- Duhamel, J.-R., Colby, C. L., & Goldberg, M. E. (1992a). The updating of the representation of visual space in parietal cortex by intended eye movements. *Science*, 255(5040), 90–92.
- Duhamel, J.-R., Goldberg, M. E., FitzGibbon, E. J., Sirigu, A., & Grafman, J. (1992b). Saccadic dysmetria in a patient with a right frontoparietal lesion. The importance of corollary discharge for accurate spatial behaviour. *Brain: a Journal of Neurology*, 115, 1387–1402. <https://doi.org/10.1093/brain/115.5.1387>.
- Dunkley, B. T., Baltaretu, B., & Crawford, J. D. (2016). Trans-saccadic interactions in human parietal and occipital cortex during the retention and comparison of object orientation. *Cortex; a Journal Devoted To the Study of the Nervous System and Behavior*, 82, 263–276. <https://doi.org/10.1016/j.cortex.2016.06.012>.
- Edelman, G. M., & Gally, J. A. (2001). Degeneracy and complexity in biological systems. *Proceedings of the National Academy of Sciences of the United States of America*, 98(24), 13763–13768. <https://doi.org/10.1073/pnas.231499798>.
- Fabius, J. H., Fracasso, A., Nijboer, T. C. W., & Van der Stigchel, S. (2019). Time course of spatiotopic updating across saccades. *Proceedings of the National Academy of Sciences of the United States of America*, 116(6), 2027–2032. <https://doi.org/10.1073/pnas.1812210116>.
- Fabius, J. H., Fracasso, A., & Van der Stigchel, S. (2016). Spatiotopic updating facilitates perception immediately after saccades. *Scientific Reports*, 6, 34488. <https://doi.org/10.1038/srep34488>.

- Fairhall, S. L., Schwarzbach, J., Lingnau, A., Van Koningsbruggen, M. G., & Melcher, D. (2017). Spatiotopic updating across saccades revealed by spatially-specific fMRI adaptation. *Neuroimage*, 147(November 2016), 339–345. <https://doi.org/10.1016/j.neuroimage.2016.11.071>.
- Hallett, P. E., & Lightstone, A. D. (1976). Saccadic eye movements to flashed targets. *Vision Research*, 16(1), 107–114. [https://doi.org/10.1016/0042-6989\(76\)90084-5](https://doi.org/10.1016/0042-6989(76)90084-5).
- Heide, W., Blankenburg, M., Zimmermann, E., & Kömpf, D. (1995). Cortical control of double-step saccades: Implications for spatial orientation. *Annals of Neurology*, 38(5), 739–748.
- Kleiner, M., Brainard, D., Pelli, D. G., Ingling, A., Murray, R., & Broussard, C. (2007). What's new in Psychtoolbox-3? *Perception*, 36(14), 1.
- Medendorp, W. P., Goltz, H. C., Vilis, T., & Crawford, J. D. (2003). Gaze-centered updating of visual space in human parietal cortex. *Journal of Neuroscience*, 23(15), 6209–6214.
- Merriam, E. P., Genovese, C. R., & Colby, C. L. (2003). Spatial updating in human parietal cortex. *Neuron*, 39(2), 361–373. [https://doi.org/10.1016/S0896-6273\(03\)00393-3](https://doi.org/10.1016/S0896-6273(03)00393-3).
- Mirpour, K., & Bisley, J. W. (2016). Remapping, spatial stability, and temporal continuity: From the pre-saccadic to postsaccadic representation of visual space in LIP. *Cerebral Cortex*, 26(7), 3183–3195. <https://doi.org/10.1093/cercor/bhv153>.
- Morris, A. P., & Krekelberg, B. (2019). A stable visual world in primate primary visual cortex. *Current Biology*, 29(9), 1471–1480. <https://doi.org/10.1016/j.cub.2019.03.069>. e6.
- Nyström, M., & Holmqvist, K. (2010). An adaptive algorithm for fixation, saccade, and glissade detection in eyetracking data. *Behavior Research Methods*, 42(1), 188–204. <https://doi.org/10.3758/BRM.42.1.188>.
- Ostendorf, F., Liebermann, D., & Ploner, C. J. (2010). Human thalamus contributes to perceptual stability across eye movements. *Proceedings of the National Academy of Sciences of the United States of America*, 107(3), 1229–1234. <https://doi.org/10.1073/pnas.0910742107>.
- Ostendorf, F., Liebermann, D., & Ploner, C. J. (2013). A role of the human thalamus in predicting the perceptual consequences of eye movements. *Frontiers in Systems Neuroscience*, 7, 10. <https://doi.org/10.3389/fnsys.2013.00010>.
- Poletti, M., Burr, D. C., & Rucci, M. (2013). Optimal multimodal integration in spatial localization. *Journal of Neuroscience*, 33(35), 14259–14268. <https://doi.org/10.1523/JNEUROSCI.0523-13.2013>.
- Price, C. J., & Friston, K. J. (2002). Degeneracy and cognitive anatomy. *Trends in Cognitive Sciences*, 6(10), 416–421. [https://doi.org/10.1016/S1364-6613\(02\)01976-9](https://doi.org/10.1016/S1364-6613(02)01976-9).
- Rath-Wilson, K., & Guitton, D. (2015). Refuting the hypothesis that a unilateral human parietal lesion abolishes saccade corollary discharge. *Brain*, 1–16. <https://doi.org/10.1093/brain/awv275>.
- Rorden, C., & Brett, M. (2000). Stereotaxic display of brain lesions. *Behavioural Neurology*, 12(4), 191–200.
- Russell, C., Deidda, C., Malhotra, P., Crinion, J. T., Merola, S., & Husain, M. (2010). A deficit of spatial remapping in constructional apraxia after right-hemisphere stroke. *Brain*, 133(4), 1239–1251. <https://doi.org/10.1093/brain/awq052>.
- Schütt, H. H., Harmeling, S., Macke, J. H., & Wichmann, F. A. (2016). Painfree and accurate Bayesian estimation of psychometric functions for (potentially) overdispersed data. *Vision Research*, 122, 105–123. <https://doi.org/10.1016/j.visres.2016.02.002>.
- Sommer, M. A., & Wurtz, R. H. (2002). A pathway in primate brain for internal monitoring of movements. *Science*, 296(5572), 1480–1482. <https://doi.org/10.1126/science.1069590>.
- Sommer, M. A., & Wurtz, R. H. (2006). Influence of the thalamus on spatial visual processing in frontal cortex. *Nature*, 444, 374–377. <https://doi.org/10.1038/nature05279>.
- Sommer, M. A., & Wurtz, R. H. (2008). Brain circuits for the internal monitoring of movements. *Annual Review of Neuroscience*, 31(1), 317–338. <https://doi.org/10.1146/annurev.neuro.31.060407.125627>.
- Sparks, D. L., & Mays, L. E. (1983). Spatial localization of saccade targets. I. Compensation for stimulation-induced perturbations in eye position. *Journal of Neurophysiology*, 49(1), 45–63. <https://doi.org/10.1152/jn.1983.49.1.45>.
- Sparks, D. L., Mays, L. E., & Porter, J. D. (2017). Eye movements induced by pontine stimulation: Interaction with visually triggered saccades. *Journal of Neurophysiology*, 58(2), 300–318. <https://doi.org/10.1152/jn.1987.58.2.300>.
- Steinbach, M. J. (1987). Proprioceptive knowledge of eye position. *Vision Research*, 27(10), 1737–1744. [https://doi.org/10.1016/0042-6989\(87\)90103-9](https://doi.org/10.1016/0042-6989(87)90103-9).
- Subramanian, J., & Colby, C. L. (2014). Shape selectivity and remapping in dorsal stream visual area LIP. *Journal of Neurophysiology*, 111(3), 613–627. <https://doi.org/10.1152/jn.00841.2011>.
- Sun, L. D., & Goldberg, M. E. (2016). Corollary discharge and oculomotor proprioception: Cortical mechanisms for spatially accurate vision. *Annual Review of Vision Science*, 2(1), 61–84. <https://doi.org/10.1146/annurev-vision-082114-035407>.
- Thaler, L., Schütz, A. C., Goodale, M. A., & Gegenfurtner, K. R. (2013). What is the best fixation target? The effect of target shape on stability of fixational eye movements. *Vision Research*, 76, 31–42. <https://doi.org/10.1016/j.visres.2012.10.012>.
- Tolias, A. S., Moore, T., Smirnakis, S. M., Tehovnik, E. J., Siapas, A. G., & Schiller, P. H. (2001). Eye movements modulate visual receptive fields of V4 neurons. *Neuron*, 29(3), 757–767. [https://doi.org/10.1016/S0896-6273\(01\)00250-1](https://doi.org/10.1016/S0896-6273(01)00250-1).
- Tzourio-Mazoyer, N., Landeau, B., Papathanassiou, D., Crivello, F., Etard, O., Delcroix, N., et al. (2002). Automated anatomical labeling of activations in SPM using a macroscopic anatomical parcellation of the MNI MRI single-subject brain. *Neuroimage*, 15(1), 273–289. <https://doi.org/10.1006/NIMG.2001.0978>.
- Umeno, M. M., & Goldberg, M. E. (1997). Spatial processing in the monkey frontal eye field. I. Predictive visual responses. *Journal of Neurophysiology*, 78, 1373–1383.
- van Doorn, J., Ly, A., Marsman, M., & Wagenmakers, E. J. (2018). Bayesian inference for Kendall's rank correlation coefficient. *American Statistician*, 72(4), 303–308. <https://doi.org/10.1080/00031305.2016.1264998>.
- von Holst, E., & Mittelstaedt, H. (1950). Das reafferenzprinzip. (Wechselwirkungen zwischen Zentralnervensystem und Peripherie). *Die Naturwissenschaften*, 37, 464–476.
- Vuilleumier, P., Sergent, C., Schwartz, S., Valenza, N., Girardi, M., Husain, M., et al. (2007). Impaired perceptual memory of locations across gaze-shifts in patients with unilateral spatial neglect. *Journal of Cognitive Neuroscience*, 19(8), 1388–1406. <https://doi.org/10.1162/jocn.2007.19.8.1388>.
- Walker, M. F., Fitzgibbon, E. J., & Goldberg, M. E. (1995). Neurons in the monkey superior colliculus predict the visual result of impending saccadic eye movements. *Journal of Neurophysiology*, 73(5), 1988–2003.
- Wichmann, F. A., & Hill, N. J. (2001). The psychometric function: I. Fitting, sampling, and goodness of fit. *Perception and Psychophysics*, 63(8), 1293–1313. <https://doi.org/10.3758/BF03194544>.
- Wurtz, R. H. (2008). Neuronal mechanisms of visual stability. *Vision Research*, 48(20), 2070–2089. <https://doi.org/10.1016/j.visres.2008.03.021>.
- Xu, Y., Wang, X., Peck, C., & Goldberg, M. E. (2011). The time course of the tonic oculomotor proprioceptive signal in area 3a of somatosensory cortex. *Journal of Neurophysiology*, 106(1), 71–77. <https://doi.org/10.1152/jn.00668.2010>.
- Zhang, G. L., Li, A. S., Miao, C. G., He, X., Zhang, Y., & Zhang, M. (2018). A consumer-grade LCD monitor for precise visual stimulation. *Behavior Research Methods*, 1–7. <https://doi.org/10.3758/s13428-018-1018-7>.